The 14-3-3 gene *par-5* is required for germline development and DNA damage response in *Caenorhabditis elegans*

David Aristizábal-Corrales[1,2], Laura Fontrodona[3], Montserrat Porta-de-la-Riva[3], Angel Guerra-Moreno[1,2], Julián Cerón[3,*] and Simo Schwartz Jr[1,2,*]

[1]Drug Delivery and Targeting, CIBBIM-Nanomedicine, Vall d'Hebron Research Institute, Universidad Autónoma de Barcelona, Barcelona 08035, Spain
[2]Networking Research Center on Bioengineering, Biomaterials and Nanomedicine (CIBER-BBN), Barcelona 08193, Spain
[3]Bellvitge Biomedical Research Institute (IDIBELL), L'Hospitalet de Llobregat, Barcelona 08908, Spain
*Authors for correspondence (sschwartz@ir.vhebron.net; jceron@idibell.org)

Summary

14-3-3 proteins have been extensively studied in organisms ranging from yeast to mammals and are associated with multiple roles, including fundamental processes such as the cell cycle, apoptosis and the stress response, to diseases such as cancer. In *Caenorhabditis elegans*, there are two 14-3-3 genes, *ftt-2* and *par-5*. *ftt-2* is expressed only in somatic lineages, whereas *par-5* expression is detected in both soma and germline. During early embryonic development, *par-5* is necessary to establish cell polarity. Although it is known that *par-5* inactivation results in sterility, the role of this gene in germline development is poorly characterized. In the present study, we used a *par-5* mutation and RNA interference to characterize *par-5* functions in the germline. The lack of *par-5* in germ cells caused cell cycle deregulation, the accumulation of endogenous DNA damage and genomic instability. Moreover, *par-5* was required for checkpoint-induced cell cycle arrest in response to DNA-damaging agents. We propose a model in which PAR-5 regulates CDK-1 phosphorylation to prevent premature mitotic entry. This study opens a new path to investigate the mechanisms of 14-3-3 functions, which are not only essential for *C. elegans* development, but have also been shown to be altered in human diseases.

Key words: 14-3-3, *par-5*, *C. elegans*, Germline, DNA damage response, Checkpoint, *wee-1.3*, *cdc-25.1*, *cdk-1*

Introduction

14-3-3 proteins are an evolutionarily conserved family implicated in diverse cellular processes, such as apoptosis or cell cycle regulation, that are associated with pathologies such as cancer (Fig. 1A) (Porter et al., 2006; Tzivion et al., 2006). They bind mainly to serine phosphorylated motifs of other proteins and regulate their subcellular localizations, stability or activity. In mammals, there are seven 14-3-3 proteins corresponding to the isoforms encoded by individual genes (designated β, γ, ε, η, σ, τ or ζ). This redundancy has hindered the study of their cellular functions, and there is still little knowledge about the consequences of 14-3-3 misfunction at the organism level (Porter et al., 2006).

14-3-3 proteins are necessary for proper cell cycle arrest following DNA damage in yeast, flies and mammals (Hermeking and Benzinger, 2006). This function is mediated by interactions with several cell cycle regulators, including Chk1 (Chen et al., 1999; Dunaway et al., 2005), Cdc25 (Kumagai and Dunphy, 1999; Lopez-Girona et al., 1999) and Cdks (Laronga et al., 2000). Checkpoint-related functions for this protein family were first discovered in fission yeast, where two 14-3-3 proteins, namely Rad24 and Rad25, regulate the G2–M checkpoint by controlling Cdc25 and Chk1 localization (Ford et al., 1994; Lopez-Girona et al., 1999; Dunaway et al., 2005). In *Drosophila melanogaster*, two 14-3-3 proteins (ζ and ε) function in cell cycle regulation during development by inhibiting entry into mitosis through the inactivation of Cdk-1 activity (Su et al., 2001). Such 14-3-3 function in controlling M-phase entry is conserved in mammals, but the contribution of each isoform separately is still under exploration.

The *Caenorhabditis elegans* germline is a powerful model for the study of the genes involved in cell cycle regulation and DNA damage response (DDR) (Gartner et al., 2004). In the *C. elegans* germline, exposure to DNA-damaging agents [e.g. ionizing radiation (IR) or ultraviolet C light] and replicative stress [e.g. hydroxyurea (HU)] triggers the checkpoint response through conserved pathways (Fig. 1B). This response leads to cell cycle arrest in the proliferative region and, in some cases (e.g. after IR), also to an increase in the proportion of apoptotic cells in the late pachytene region of the germline. The underlying DDR molecular pathway, conserved from yeast to mammals, acts through the ATL-1 and ATM-1 kinases (ATR and ATM homologs) (Garcia-Muse and Boulton, 2005) as well as several sensor proteins, such as HUS-1 (Hofmann et al., 2002), MRE-11 (Garcia-Muse and Boulton, 2005) and WRN-1 (Lee et al., 2010). CHK-1 and CHK-2, are the effector kinases (Kalogeropoulos et al., 2004; Stergiou et al., 2007; Bailly et al., 2010; Lee et al., 2010), but other proteins, such as RAD-5, act in parallel with this canonical pathway to promote checkpoint responses (Ahmed et al., 2001; Collis et al., 2007).

In *C. elegans*, two 14-3-3 genes, *par-5* (also named *ftt-1*) and *ftt-2*, encode 14-3-3 proteins, and these share 86% of the amino
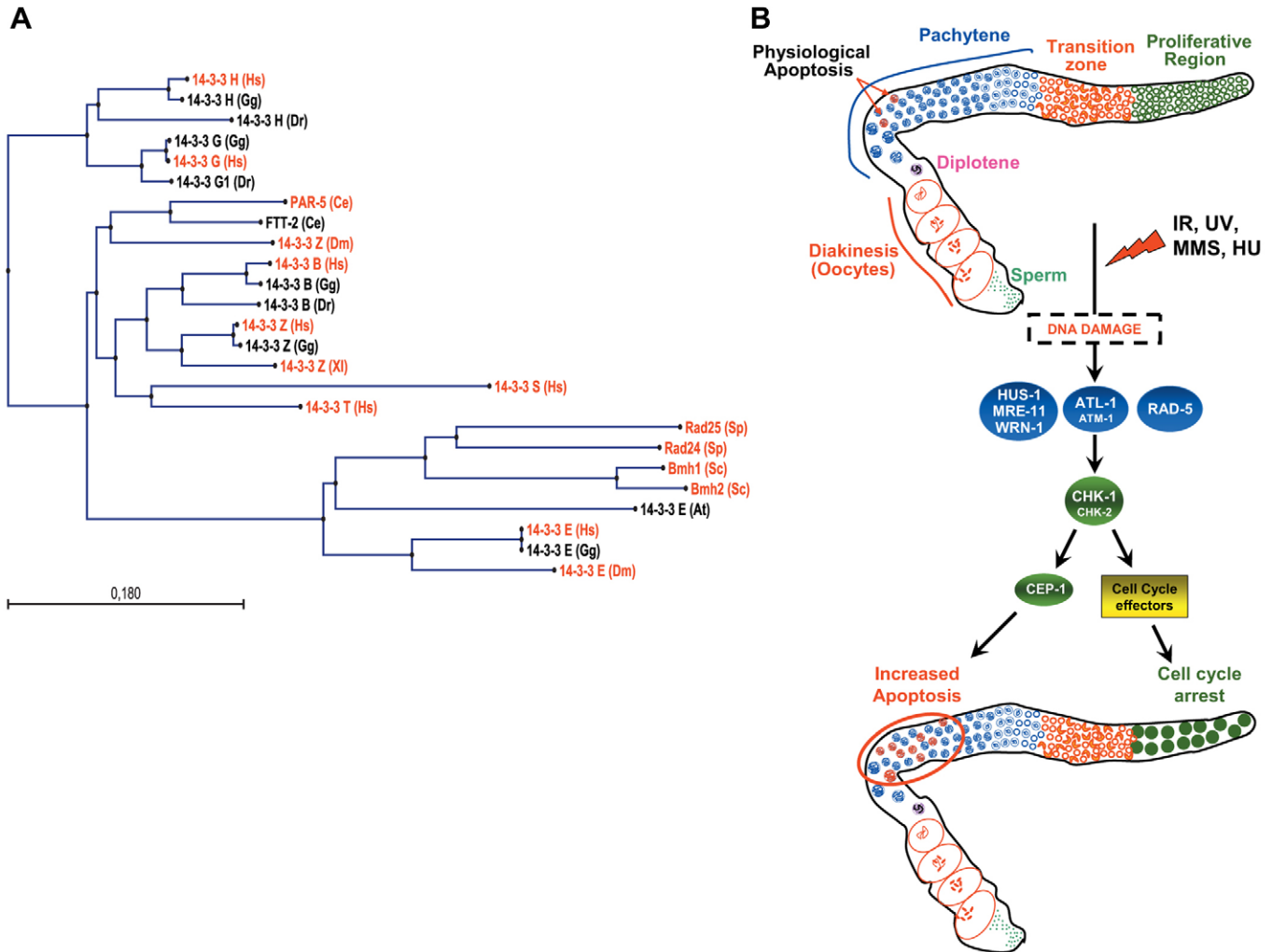
Fig. 1. Phylogenetic tree of 14-3-3 family proteins and the DNA damage response in the *Caenorhabditis elegans* germline. (**A**) 14-3-3 ortholog sequences were aligned using ClustalW, and CLC Sequence Viewer was used to generate the tree using the Neighbor Joining algorithm. Names in red correspond to 14-3-3 members, which have been either related to cell cycle control or shown to interact physically with checkpoint and/or cell cycle proteins (Hermeking and Benzinger, 2006). At, *Arabidopsis thaliana*; Ce, *C. elegans*; Dm, *Drosophila melanogaster*; Dr, *Danio rerio*; Gg, *Gallus gallus*; Hs, *Homo sapiens*; Sc, *Saccharomyces cerevisiae*; Sp, *Schizosaccharomyces pombe*; and Xl, *Xenopus laevis*. (**B**) The upper part of the figure shows germline organization in the adult worm stage. In the distal germline, cells proliferate to produce new germ cell precursors (green zone). Next, cells abandon the proliferative region to pass into the transition zone (in orange) before starting the meiotic phase (in blue) to give rise finally to the oocytes in the most proximal region (diakinesis stage). During development many meiotic cells are eliminated by physiological apoptosis. After the induction of DNA damage by different agents, a checkpoint response is activated in the germline. DNA damage induces a molecular response pathway that includes several conserved transducer and effector proteins, as shown in the middle of the figure. The activation of this pathway is reflected in two germline phenotypes: cell cycle arrest in the proliferative region and, in some cases, an increase in apoptotic cells in the pachytene region (bottom of the figure).

acid sequence. Despite this high identity, the expression pattern is distinct because only PAR-5 is expressed in the germline (Wang and Shakes, 1997). *Caenorhabditis elegans* 14-3-3 proteins have been linked to lifespan extension and the stress response (upon oxidative and heat stimuli) by interacting with SIR2.1 deacetylase and the forkhead transcription factor, DAF-16 (Berdichevsky et al., 2006). However, this role has not been ascribed to *par-5* (Li et al., 2007).

par-5 belongs to the partitioning defective PAR family, which regulates the asymmetry in the first embryonic cell division. During this process, *par-5* is required for the proper distribution of asymmetrically localized PAR proteins (Morton et al., 2002). Uniquely for a PAR protein, PAR-5 is homogeneously distributed

in the embryo and so studies of the asymmetric cell division mechanism have focused on other members of the PAR family (Suzuki and Ohno, 2006). Intriguingly, PAR-5 is also present in the adult germline (Morton et al., 2002), but its function in germ cells remains unknown. Despite the conservation of 14-3-3 checkpoint-related functions from yeast to mammals, this study is the first to provide evidence of a role in DDR for a 14-3-3 protein in the key model organism *C. elegans*.

Results

par-5 is required for proper germline development

par-5 mutations or *par-5* RNA interference (RNAi)-mediated knockdown [*par-5(RNAi)*] produces low brood size, embryonic

lethality and sterility (Morton et al., 2002). However, although the role of *par-5* in embryonic development has been established, its function in the adult germline is poorly understood. To investigate the role of *par-5* in the adult germline, we studied phenotypes in the *par-5* mutants *it55* (allele with a single amino acid substitution that reduces the protein expression level) (Morton et al., 2002) and *par-5(RNAi)* worms. In the 1-day adult stage, the number of germ cells and gonad size were reduced in the mutant strain, and such a reduction was found not to be temperature dependent (supplementary material Fig. S1). This germline proliferation defect was even more pronounced in *par-5* RNAi-fed worms (Fig. 2A). In contrast to wild type (WT) and *par-5* mutants, *par-5(RNAi)* germlines showed some small fragmented nuclei, indicating mitotic catastrophe and genome instability in the proliferative region. By performing a time-course analysis of the germline development, we found that the proliferative defect in *par-5*-defective worms started at the L4 stage when hypercondensed and fragmented nuclei become apparent. After this stage, the number of germ cells decreased in *par-5(RNAi)* germlines in contrast to the continuous proliferation observed in the WT and *par-5(it55)* (Fig. 2B). Despite the important reduction in germ cells in *par-5(it55)* worms, nuclei fragmentation was not as abundant in *par-5* mutants as it was in

par-5(RNAi) animals (Fig. 2A). The difference between *par-5(it55)* and *par-5(RNAi)* phenotypes implies that the *it55* allele is hypomorphic rather than null (Morton et al., 2002). Indeed, *par-5(it55)* fed with *par-5* RNAi presented a *par-5(RNAi)* phenotype (Fig. 2A).

The germline proliferation defect observed after *par-5* knockdown could be explained by the influence of the somatic gonad on germline proliferation (Killian and Hubbard, 2005). However, *par-5* RNAi treatment in the *rrf-1(pk1417)* background (a strain with defective RNAi in somatic cells) showed the same germline phenotype as that of WT animals (supplementary material Fig. S2). Therefore, the *par-5* knockdown effect on the germline is independent of the somatic functions of *par-5*. Additionally, most of the *par-5(RNAi)* gonads showed either a reduction in the number, or an absence, of oocytes. This observation suggests that *par-5* is implicated not only in germline proliferation, but also in meiotic progression, which is in agreement with the meiotic arrest phenotype previously described (Morton et al., 2002).

par-5 shares ~80% homology with *ftt-2*, which is the other 14-3-3 *C. elegans* gene (Wang and Shakes, 1997). To test whether the observed RNAi phenotype was *par-5* specific, we quantified *par-5* and *ftt-2* transcript levels using quantitative RT-PCR after
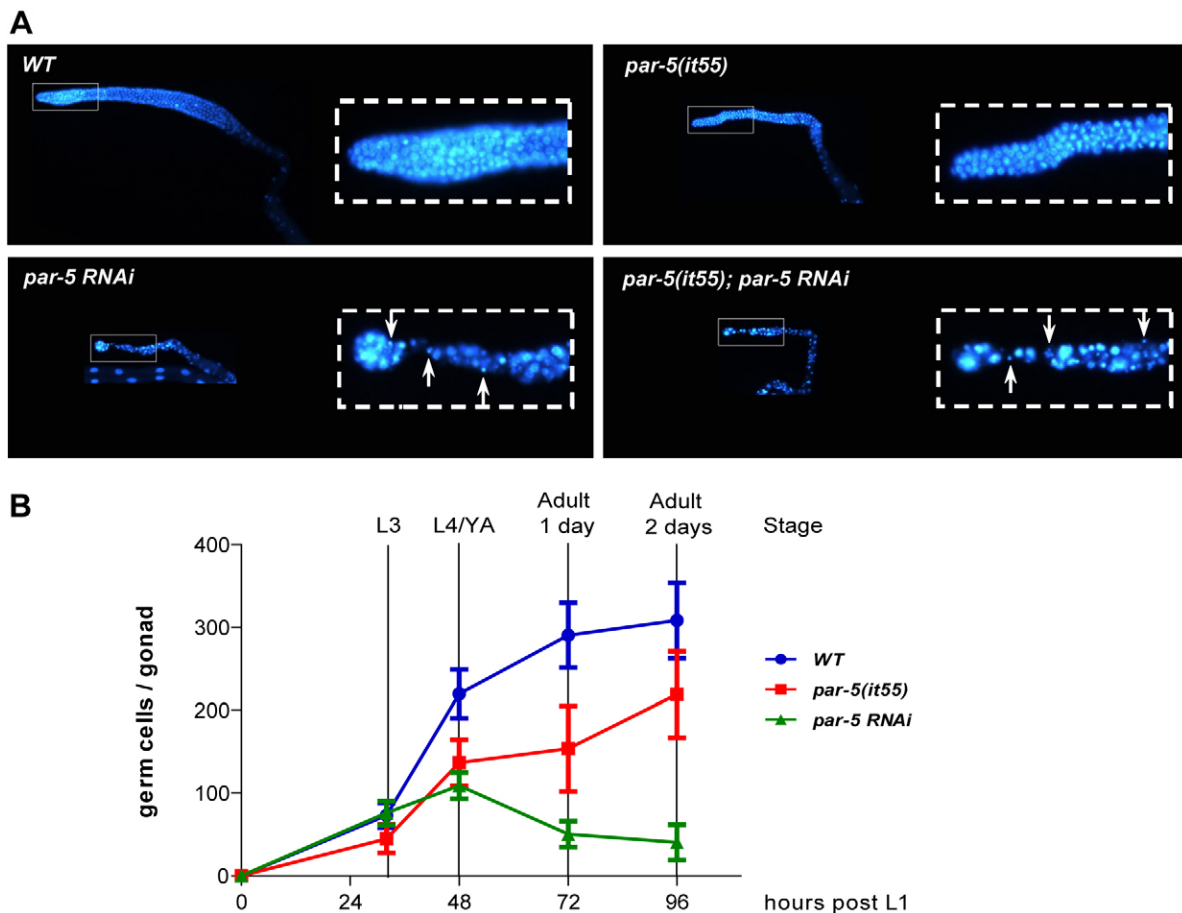

Fig. 2. *par-5* inactivation affects germline proliferation. (A) Representative images of DAPI-stained germlines from WT or *par-5(it55)* mutant worms (1-day-old adults) fed with *par-5* RNAi or the RNAi empty vector. The proliferative regions of germlines are shown enlarged in rectangles. Arrows indicate hypercondensed and fragmented nuclei. **(B)** Graph showing the number of germ cells per gonad at different developmental stages for WT, *par-5(it55)* and *par-5* RNAi-fed worms. L1 larvae grown at 20℃ were fixed and stained with DAPI at the indicated times. Error bars indicate standard deviations from the mean.

par-5 RNAi treatment. This experiment showed that *par-5* RNAi depleted *par-5* mRNA, whereas *ftt-2* transcript levels were unaffected (supplementary material Fig. S3). All these observations indicate that *par-5* is required for the proliferation, genomic stability and meiotic progression of the germline.

Inactivation of *par-5* promotes endogenous DNA damage accumulation

Because we found a reduced number of germ cells and DNA fragmentation after *par-5* inactivation by RNAi (Fig. 2A), we further investigated the role of *par-5* in the maintenance of DNA

stability. We examined the abundance of RAD-51 foci, which acts as a marker of processed double-strand breaks (DSBs) and stalled replication forks (Alpi et al., 2003; Ward et al., 2007). Interestingly, we observed a tenfold increase in the number of RAD-51 foci at the proliferative region of *par-5(RNAi)* worms (Fig. 3A,B; supplementary material Fig. S10). This increase is similar to that obtained with the checkpoint defective strain *atl-1(tm853)* (Garcia-Muse and Boulton, 2005).

To corroborate the role of *par-5* in preserving genomic stability, we used a transgenic strain expressing the fusion protein HUS-1::GFP, which is a DNA damage sensor protein that forms
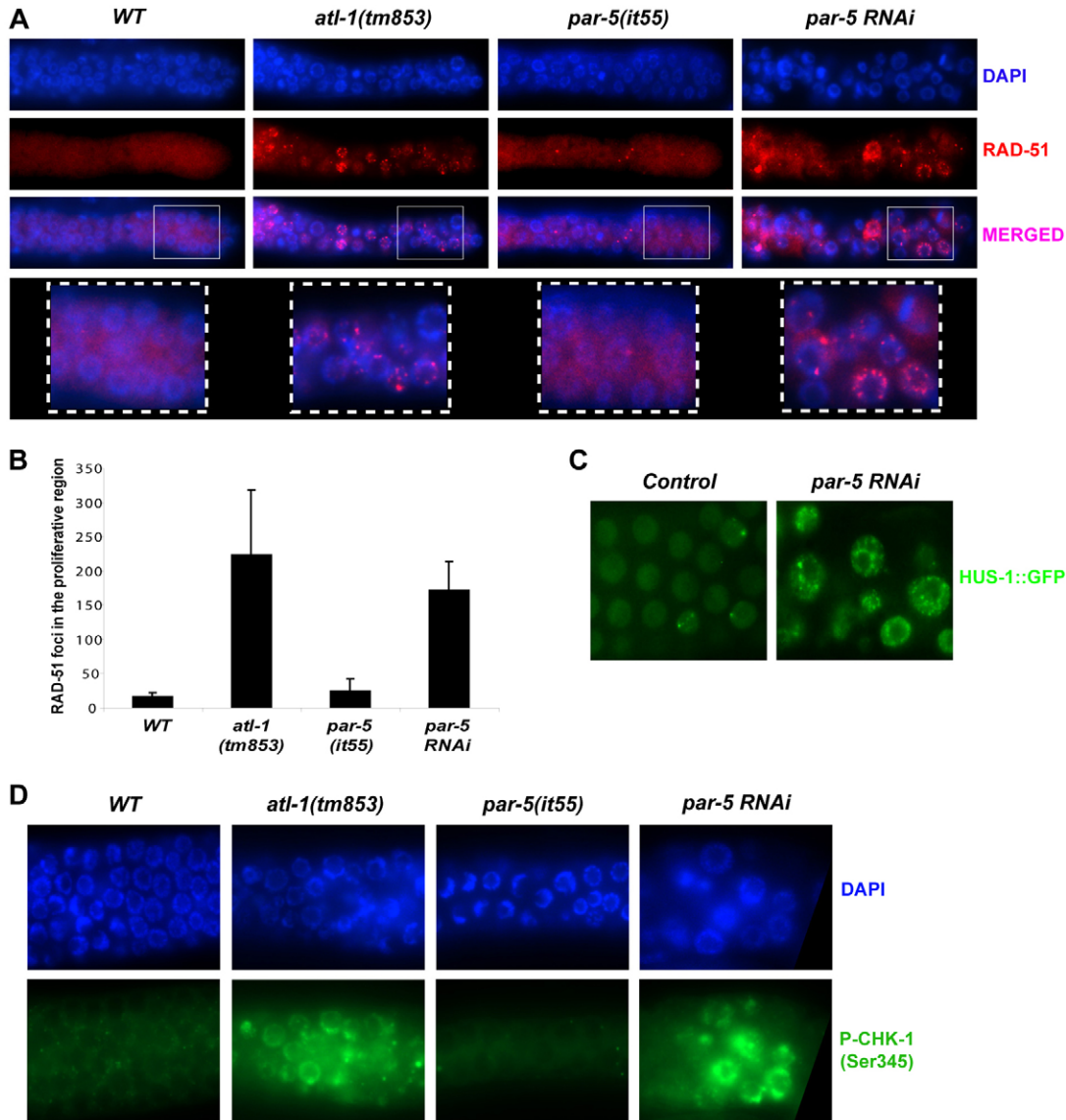

Fig. 3. Lack of *par-5* results in DNA damage accumulation and CHK-1 activation. (A) *par-5* suppression promotes RAD-51 accumulation. Representative images of the germline proliferative regions from worms of the indicated genotypes and/or RNAi, immunostained with a RAD-51 antibody and counterstained with DAPI. Distal proliferative regions enlarged in squares show the RAD-51 foci nuclear localization. **(B)** The graph shows RAD-51 foci quantification in all the stacks within 30 μm of the distal end of the gonad. Error bars indicate the standard deviation of the mean from at least 15 germlines for each experiment. **(C)** HUS-1::GFP foci increase after *par-5* knockdown. Representative images of the meiotic germ cells from a transgenic strain expressing a HUS-1::GFP fusion protein with or without *par-5* RNAi treatment. **(D)** CHK-1 phosphorylation is detected in pre-meiotic germ cells after *par-5* RNAi knockdown. Representative images of the pre-meiotic germ cells (cells between the proliferating and the transition region) from the worms of the indicated genotypes/RNAi, immunostained with a phosphorylated CHK-1 (Ser345) antibody and counterstained with DAPI. The percentage of germlines positively stained (at least 4–5 stained germ cells per gonad) with phosphorylated CHK-1 was: 5% for WT, 50% for *atl-1(tm853)*, 10% for *par-5(it55)* and 75% for *par-5* RNAi.

defined foci at DSBs (Hofmann et al., 2002). The meiotic region of WT animals showed a few HUS-1::GFP foci as a result of transient DSBs that occurred during meiotic recombination. However, *par-5* RNAi showed a marked increase in the number of HUS-1::GFP foci, indicating a higher accumulation of DSBs (Fig. 3C). These results link *par-5* with the DDR pathway.

In addition to the increase in DNA damage markers (RAD-51 and HUS-1 foci), *par-5(RNAi)* worms showed constitutive phosphorylation of the checkpoint kinase CHK-1 (at Serine 345) in germ cells localized at the proximal side of the proliferative region (Fig. 3D; supplementary material Fig. S11). This modification has been associated with recombination defects that trigger meiotic checkpoint activation (Jaramillo-Lambert et al., 2007). Notably, the same pattern was also observed in the *atl-1(tm853)* strain, whereas this phenotype was rarely present in WT worms and *par-5(it55)* mutants. Therefore, the RNAi depletion of *par-5* seems to cause pre-meiotic checkpoint activation similar to the effect of inactivating genes that control DNA stability, such as *atl-1*. Taken together, these results suggest that *par-5* is necessary for proper DNA maintenance because its inhibition promotes DNA damage accumulation both in proliferating and meiotic germ cells.

par-5 function is necessary for S and G2–M checkpoint responses

The accumulation of RAD-51 foci and the nuclei fragmentation observed in the proliferative region of *par-5* RNAi germlines (Fig. 2A, Fig. 3A) resemble the effect of mutations on the genes of the checkpoint pathway, such as *atl-1* and *chk-1* (Kalogeropoulos et al., 2004; Garcia-Muse and Boulton, 2005). Thus, we tested whether *par-5* is actively implicated in the DDR under replication stress induced by HU. HU inhibits the activity of the ribonucleotide reductase enzyme, causing the depletion of deoxyribonucleotide triphosphate (dNTP) levels and so hampering DNA replication (Kim et al., 1967). After HU treatment, cells in the proliferative region of the germline arrested in the S-phase as a result of checkpoint activation. This cell cycle arrest was evidenced by fewer nuclei with larger sizes (Gartner et al., 2004). Interestingly, after HU treatment, these checkpoint response marks were absent in *par-5(RNAi)* worms and *par-5(it55)* mutants (Fig. 4A). Such incapacity to arrest the cell cycle after HU treatment was also observed in mutants for the checkpoint gene *atl-1*.

The *C. elegans* embryo is another scenario in which the checkpoint response induced by replication stress has been widely studied. In particular, the presence of HU causes a delay in the mitotic entry at the first embryonic division (Brauchle et al., 2003). Through video recordings of the first embryonic division, we observed that *par-5(RNAi)* and *par-5(it55)* embryos rescued the HU-induced cell cycle delay (supplementary material Fig. S4). Therefore, *par-5* is also required for the embryonic DNA replication checkpoint, as are other checkpoint genes previously described (Brauchle et al., 2003; Moser et al., 2009).

To clarify whether the checkpoint role of *par-5* is exclusive for the S-phase, we investigated its role in the IR-induced G2–M checkpoint. *par-5(RNAi)* and *par-5* mutant germ cells bypassed the cell cycle arrest induced by IR and showed some fragmented and hypercondensed nuclei (Fig. 4B). These experiments indicate that *par-5* is an essential gene for cell cycle arrest in response to diverse exogenous insults, participating in both the S and the G2–M checkpoints.

par-5 prevents premature entry into mitosis

While testing the germline response to HU after *par-5* inhibition, we observed many germ nuclei that presented hypercondensed chromatin and smaller sizes (Fig. 4A). This effect, observed both in *par-5(RNAi)* and in *par-5(it55)* animals, was likely to be because of cells entering prematurely into mitosis before the DNA was properly replicated, thereby causing DNA fragmentation. To study this phenotype, we used an antibody against phosphorylated histone 3 (H3) as a mitotic marker (Fig. 4C). Although the number of mitotic germ cells was reduced in WT animals as a result of the S-phase checkpoint activation, the inactivation of *par-5* (either by RNAi or mutation) caused an increase in the number of mitotic cells after HU treatment. Therefore, this result indicates that HU-treated germ cells, in which *par-5* function is impaired, are able to enter mitosis, thereby bypassing the S-phase checkpoint. Consistently, a similar phenotype was also observed in the *atl-1(tm853)* strain.

Although *par-5* activity in controlling premature mitotic entry becomes obvious after HU treatment, we also observed a slight increase in the number of phosphorylated H3-positive cells in *par-5(RNAi)* and *par-5(it55)* unchallenged worms (Fig. 4C). Using a time-course experiment, we detected an increase in the number of mitotic figures and DNA fragmentation at the L4 stage, which is the developmental stage chosen to expose worms to HU in our checkpoint assays (supplementary material Fig. S5). All these results suggest that *par-5* is required to prevent premature entry into mitosis, both upon replicative stress and during normal germ cell proliferation. Such a function is the hallmark of checkpoint genes.

PAR-5 accumulates in germ cell nuclei after checkpoint activation

14-3-3 proteins are known to regulate the subcellular localization of their substrates in response to DNA damage (Lopez-Girona et al., 1999; Dunaway et al., 2005). To further explore the mechanism by which *par-5* acts in the checkpoint response, we examined PAR-5 expression and subcellular localization by confocal microscopy in normal and HU-treated germlines. Previous studies demonstrated that PAR-5 is expressed in the germline syncytium (Morton et al., 2002). In agreement with this, we found PAR-5 localized around the nuclei of germ cells. Interestingly, after HU treatment, we observed a large amount of PAR-5 protein inside the large S-phase-arrested nuclei (Fig. 5A). This nuclear localization could be important for its role in the DDR, because no changes in protein expression levels were observed after treatment with HU (Fig. 5B).

par-5 is required for CDK-1 phosphorylation after DNA damage

It has been demonstrated that *par-5* homologs in yeast, flies and mammals (14-3-3 proteins) regulate G2–M transition through interactions with the cell cycle regulator proteins Wee1, Cdc25 and Cdk1 (Cdc2) (Peng et al., 1997; Chan et al., 1999; Kumagai and Dunphy, 1999; Zeng and Piwnica-Worms, 1999; Laronga et al., 2000; Lee et al., 2001). As a canonical cell cycle progression mechanism, Cdc25 dephosphorylates Cdk1 to allow entry into mitosis. However, after DNA damage, Cdk1 and Cdc25 are inactivated by phosphorylation (by the Wee1 and Chk1 kinases, respectively) in a checkpoint-dependent manner, leading to cell cycle arrest. In *C. elegans*, CDK-1 is also
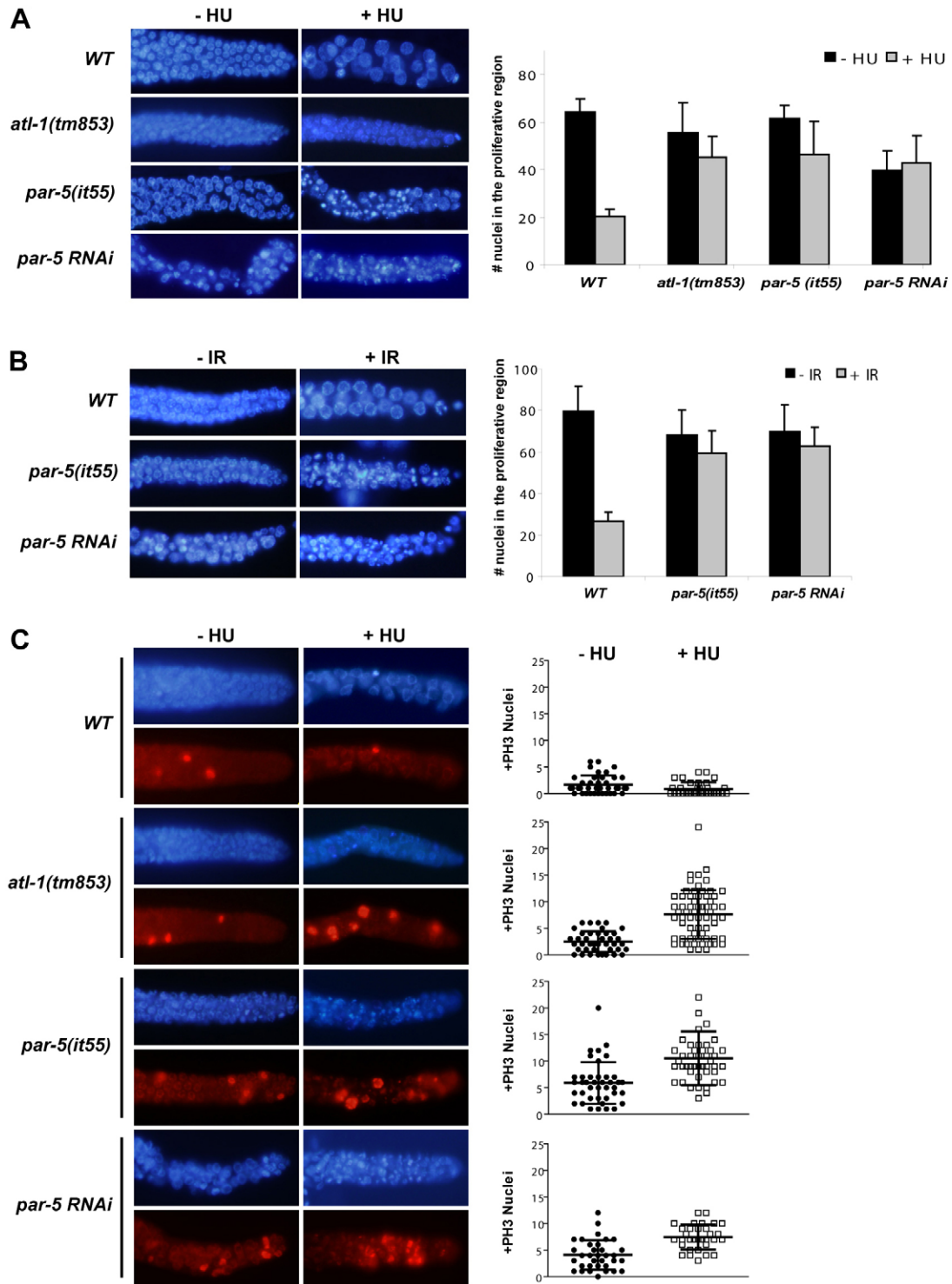
Fig. 4. Cell cycle arrest induced by DNA damage depends on *par-5* function. (**A**) *par-5* is required for HU-induced cell cycle arrest. Representative images of germline proliferative regions from the worms of the indicated genotypes and/or RNAi, treated with (+HU) or without (–HU) HU and stained with DAPI. The graph shows germ nuclei quantification. Error bars indicate standard deviations from the mean. (**B**) *par-5* is also necessary for IR-induced responses. Representative images of germline proliferative regions from the worms of the indicated genotypes and/or RNAi, irradiated (+IR) or not (–IR) with γ-rays. The graph shows germ nuclei quantification and error bars indicate standard deviations from the mean. (**C**) *par-5* inactivation leads to premature mitotic entry. Worms were treated with HU as for A, and then the germlines were immunostained with a phosphorylated H3 antibody and counterstained with DAPI. The graph shows the quantification of phosphorylated H3-positive cells in all the stacks within 50 μm of the distal end of the gonad. Error bars indicate the standard deviation of the mean from at least 30 germlines for each experiment.
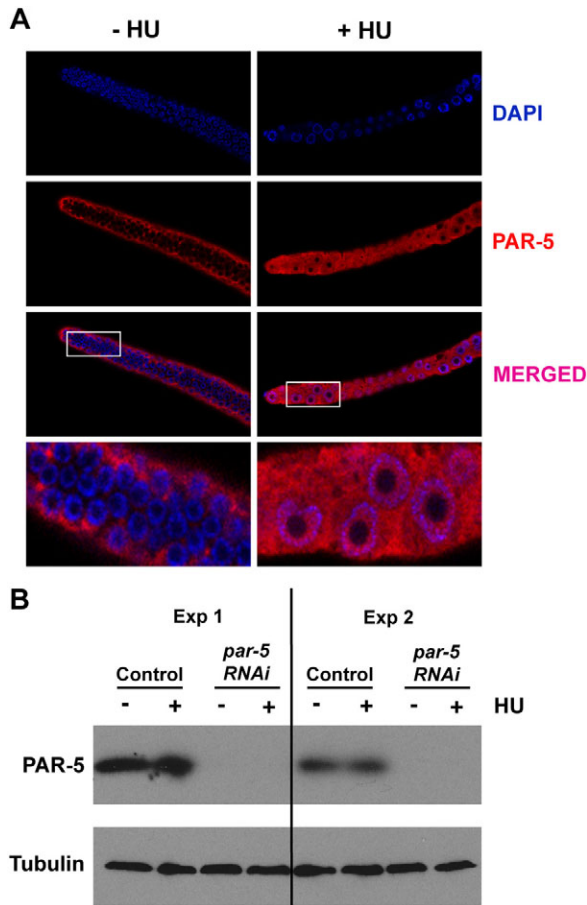
Fig. 5. PAR-5 location and expression after replication stress induced by HU. (**A**) Representative confocal images showing a single Z stack of germlines from WT worms treated with (+HU) or without (–HU) HU, immunostained with a PAR-5 antibody and counterstained with DAPI. (**B**) Protein extracts from WT worms fed with the *par-5* RNAi or the RNAi empty vector (control) and treated with (+) or without (–) HU were blotted using a PAR-5 antibody. The blotting was performed using extracts from two biological replicates.

phosphorylated in the Tyr15 inhibitory residue upon DNA damage (Moser et al., 2009; Bailly et al., 2010).

Given that we observed premature entry into mitosis in *par-5(RNAi)* and in *par-5(it55)* worms after DNA damage, we investigated whether *par-5* inactivation affected CDK-1 phosphorylation. Similar to HU, treatment with camptothecin (CPT) produced CDK-1 phosphorylation and the consequent cell cycle arrest in the proliferative region of the WT germline (Fig. 6A). However, after *par-5* RNAi knockdown, phosphorylated CDK-1 staining was strongly reduced in the proliferative region. The same effect was observed in *atl-1(tm853)* strains, suggesting that lack of phosphorylated CDK-1 is a consequence of deficient checkpoint activation. *par-5* mutants revealed some germ cells with phosphorylated CDK-1 staining after CPT treatment, reflecting the milder *par-5* inactivation compared with the *par-5(RNAi)* animals (Fig. 6A; supplementary material Fig. S12).

To further investigate the link between PAR-5 and CDK-1 phosphorylation, we examined the functional relation between *par-5* and *cdc-25.1*. In yeast and mammals, Cdc25 phosphatase

removes the Cdk1 inhibitory phosphorylation (Tyr15) to promote mitosis entry. Accordingly, we observed that *cdc-25.1* suppression enhances CDK-1 phosphorylation upon DNA damage in *C. elegans* (Fig. 6A). Moreover, *cdc-25.1* RNAi produces cell cycle arrest in the proliferative region of the germline that mimics the checkpoint response (Fig. 6B). This *cdc-25.1* RNAi phenotype effect was rescued in a *par-5(it55)* background, pointing towards an opposite function for *par-5* and *cdc-25.1* in cell cycle control. A similar antagonism to regulate the cell cycle has been described in fission yeast for Wee1 and Cdc25 (Raleigh and O'Connell, 2000). In that model, Cdk1 phosphorylation relies on the balance between the activities of the kinase Wee1 and the phosphatase Cdc25. Consequently, we assessed whether *par-5* could be acting in the same pathway as *wee-1* to counteract *cdc-25.1* function. In *C. elegans*, there are two *wee-1* genes, *wee-1.1* and *wee-1.3*. *wee-1.3* regulates *cdk-1* function in the germline (Burrows et al., 2006) and we observed that *wee-1.3* partially suppressed the *cdc-25.1* arrest phenotype (supplementary material Fig. S6). We then tested whether *wee-1.3*, similar to *par-5*, was necessary for HU-induced cell cycle arrest. As with *par-5* RNAi, *wee-1.3* knockdown inhibited the checkpoint induced by replication stress, leading to aberrant mitosis and nuclei fragmentation (Fig. 6C).

These results suggest that PAR-5 controls entry into mitosis in the same manner as does WEE-1.3 to promote CDK-1 phosphorylation and counteract CDC-25.1 function. Such a model would place PAR-5 downstream of the checkpoint pathway as part of the effector proteins required for DNA damage-induced cell cycle arrest (Fig. 7).

Discussion
The ability of 14-3-3 proteins to interact physically with many proteins offers PAR-5 the potential to be involved in several developmental processes. In this study, we dissected two separate functions for *par-5* in the germline, one in germ cell proliferation and another responding to DNA damage. Although both functions might be related and influenced by the role of *par-5* in preventing premature mitotic entry, the pathways regulating these two processes as the level of PAR-5 might be different.

par-5 and germline development
The decrease in the number of germ cells in *par-5*-defective animals could be explained, at least partially, by abnormal and uncontrolled entry into the M-phase, which leads to mitotic defects (Fig. 4C). After *par-5* knockdown, we detected some nuclei that showed hyperfragmented chromatin. These cells probably suffered mitotic catastrophe and so were unable to continue dividing, contributing to the strong decrease in germ cell precursors after *par-5* RNAi administration (Fig. 2A,B). This phenotype was rarely observed in *par-(it55)* animals, in which, although the proliferation rate was affected, reduced PAR-5 levels are sufficient to maintain the dividing of germ cells without mitotic catastrophe. The nuclei fragmentation observed in *par-5(RNAi)* germ cells was accompanied by an accumulation of RAD-51 foci in the proliferative region of the germline. Both phenotypes have previously been related to defects in the maintenance of replication stability and the consequent aberrant mitosis, which has also been observed after the suppression of key checkpoint genes, such as *atl-1*, *wrn-1* and *chk-1* (Kalogeropoulos et al., 2004; Garcia-Muse and Boulton, 2005; Lee et al., 2010). In addition, budding yeast 14-3-3 proteins negatively regulate Exo1 nuclease
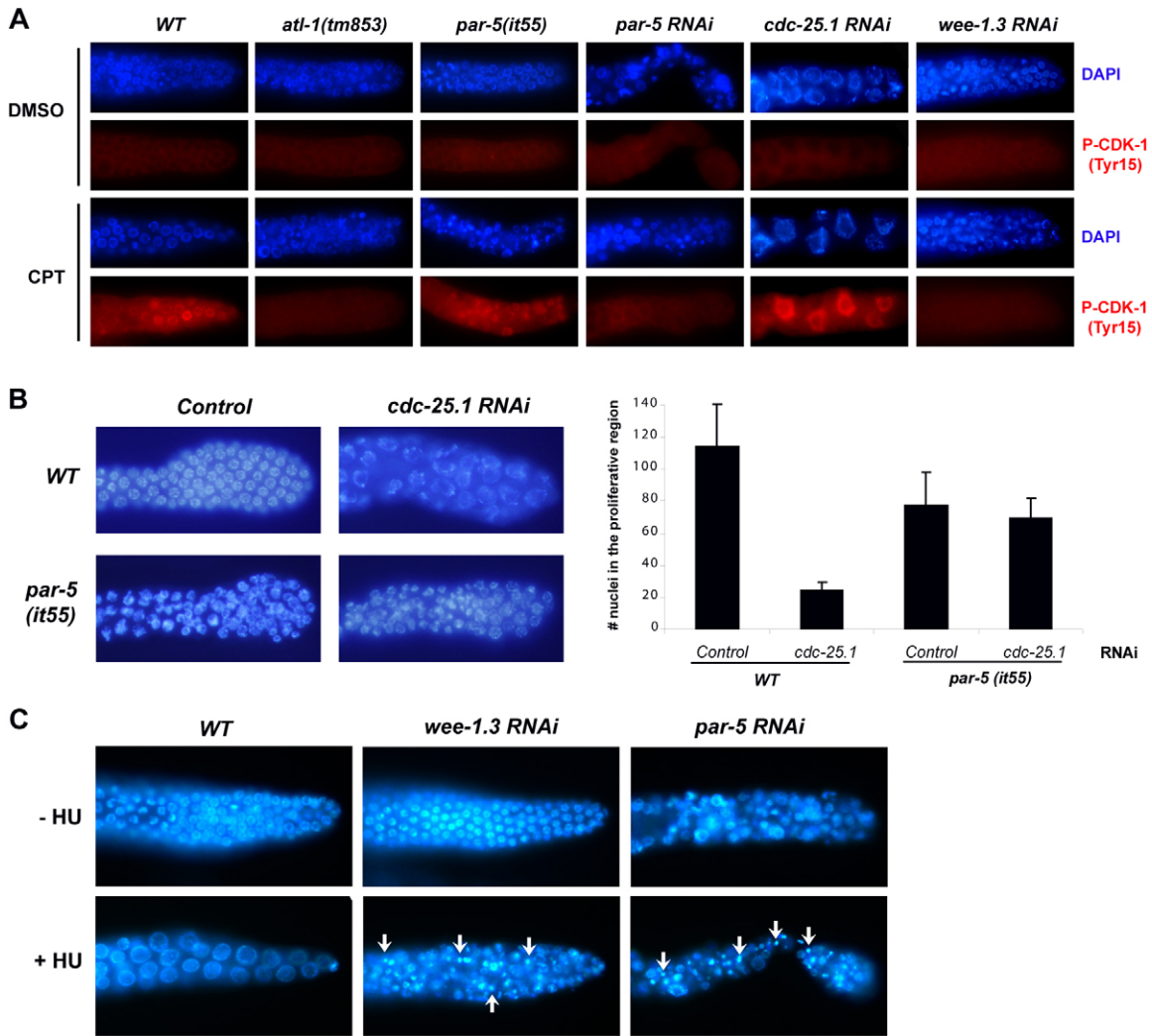
Fig. 6. ***par-5* regulates CDK-1 phosphorylation.** (**A**) *par-5* is required for CDK-1 phosphorylation after DNA damage. Representative images of germline proliferative regions from the worms of the indicated genotypes and/or RNAi, treated with CPT or vehicle control (DMSO) immunostained with a phosphorylated CDK-1 (Tyr15) antibody and counterstained with DAPI. (**B**) *par-5* counteracts *cdc-25.1* function. Representative images of the proliferative region of germlines from WT or *par-5(it55)* worms (1-day-old adults) fed with the RNAi empty vector or *cdc-25.1* RNAi (from the L3 stage) stained with DAPI. The graph shows germ nuclei quantification. Error bars indicate standard deviations from the mean. (**C**) *wee-1.3* suppression mimics *par-5* RNAi phenotype upon HU treatment. Representative images of germline proliferative regions from WT worms fed with *wee-1.3* or *par-5* RNAi, treated with (+HU) or without (–HU) HU and stained with DAPI. The nuclear fragmentation shown was observed in 90% of the *wee-1.3* and *par-5* RNAi-treated germlines.

activity, which is involved in the pathological process of stalled replication forks that produces the accumulation of single-strand DNA gaps (Engels et al., 2011). Nevertheless, it is unknown whether this interaction occurs in *C. elegans*.

The lack of oocytes observed in *par-5(RNAi)* worms also highlighted that *par-5* has a role in meiotic progression. Interestingly, after *par-5* knockdown, we observed an increase in HUS-1::GFP foci, reflecting the accumulation of unrepaired DSBs in the meiotic region. This observation, together with the accumulation of RAD-51 foci in proliferating cells, suggests that *par-5* is required to repair endogenous DNA damage. However, we cannot rule out the possibility that *par-5* depletion causes additional DNA damage (directly or indirectly) through a different mechanism. The increase in DNA damage in the germlines of *par-5(RNAi)* worms was also

accompanied by constitutive phosphorylation of CHK-1 (Ser345) in pre-meiotic germ cells. Given that we observed the same phenotype in *atl-1(tm853)* mutants, CHK-1 phosphorylation is probably mediated by ATM-1 instead of by ATL-1. In agreement with this hypothesis, it has been suggested that *atm-1* controls meiotic checkpoint activation (Bhalla, 2010; Jaramillo-Lambert et al., 2010). Both the accumulation of DSBs (HUS-1::GFP foci) and constitutive meiotic CHK-1 activation could contribute to the absence of oocytes after *par-5* RNAi, because the damaged meiotic cells might not progress to reach proper oocyte differentiation.

We conclude that the altered mitosis and meiosis observed in the germlines of *par-5*-defective worms are related to an accumulation of DNA damage in germ cells, which is compatible with the role of *par-5* in the DDR pathway.
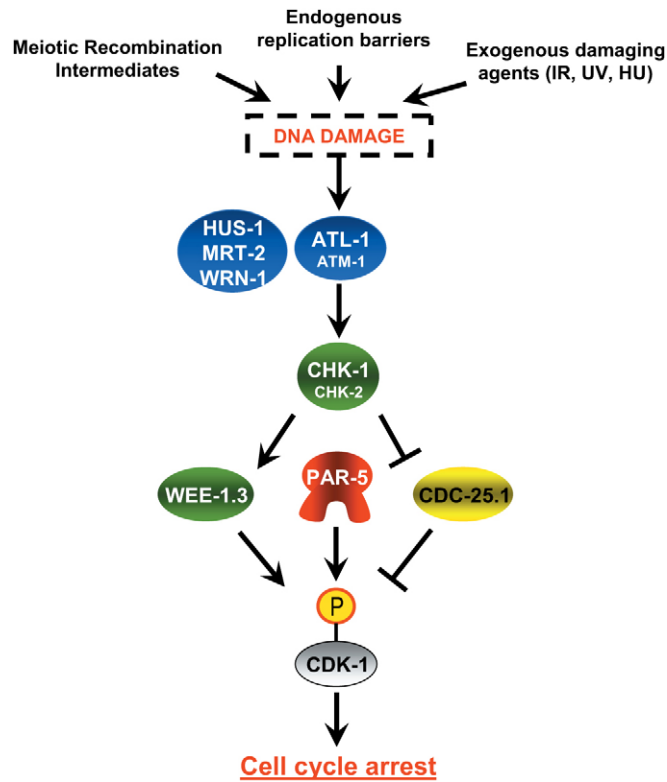
Fig. 7. Model of *par-5* function within DNA damage-induced cell cycle arrest. After the detection of endogenous or exogenous DNA damage, checkpoint sensor proteins (e.g. HUS-1 and MRT-2) activate ATL-1 and ATM-1, which in turn phosphorylate the CHK-1 and CHK-2 kinases. The contribution of ATL-1–ATM-1 and CHK-1–CHK-2 to the response depends mainly on the DNA damage that triggers the response. However, ATL-1 and CHK-1 are considered to be the main actors in the pathway. Downstream of CHK-1, the cell cycle can be arrested by promoting CDK-1 inactivation by phosphorylation. According to our results, CDK-1 phosphorylation status relies on the balance between the activities of the WEE-1.3 kinase and those of the CDC-25.1 phosphatase. Therefore, checkpoint signaling would favor WEE-1.3 activation and CDC-25.1 inhibition (which is likely to be by CHK-1-mediated phosphorylation). In this context, we propose that PAR-5 is necessary to promote and/or maintain CDK-1 phosphorylation (inactive form) and so to induce cell cycle arrest properly upon DNA damage.

Function of *par-5* within the checkpoint pathway

We demonstrated that, in *C. elegans*, the 14-3-3 gene *par-5* is required to promote proper cell cycle arrest after DNA damage. Interestingly, although only *par-5(RNAi)* worms showed endogenous DNA damage accumulation and nuclei fragmentation, both *par-5(it55)* and *par-5(RNAi)* worms presented similar checkpoint defects in response to exogenous DNA damage. Therefore, taking into account the fact that the mutant strain retains some protein expression (Morton et al., 2002), it is clear that a mild decrease in PAR-5 level is enough to affect the extrinsic DNA damage-induced checkpoint response, whereas a stronger depletion of the protein [as shown in our RNAi experiments (Fig. 5B)] affects germ cell cycle progression and DNA stability.

PAR-5 belongs to the PAR family, which controls the asymmetric first cell division in the embryo. This process includes the tight regulation of the cycling time in the posterior and anterior cells (Suzuki and Ohno, 2006). However, worms fed

with RNAi against *par-2* and *par-3* (members of the anterior and posterior complexes that drive asymmetry in the embryo) showed normal cell cycle arrest after HU treatment (supplementary material Fig. S7). Moreover, when we studied the cell cycle of the first embryonic division, we found that *par-5*-defective embryos presented a shorter S-phase and a longer M-phase (supplementary material Fig. S4). By analyzing videos from the Phenobank (http://www.worm.mpi-cbg.de/phenobank/cgi-bin/ MenuPage.py), such cell cycle alterations seem to be unique among PAR family members (supplementary material Fig. S9). These experiments indicate that participation in DDR is a rare feature of the PAR family, but one that is specific for PAR-5.

PAR-5 has also been shown to act as a target of MPK-1 (the ERK pathway) to govern pachytene cellular organization in the germline (Arur et al., 2009). As in the case of the PAR proteins examined, the inhibition of MPK-1 did not affect cell cycle arrest, even though the worms were sterile (supplementary material Fig. S7). Therefore, the role of *par-5* in DDR is unrelated to its described function in the *mpk-1* pathway, underscoring the multifunctional role of this gene.

Several 14-3-3 protein partners that could help explain the role of *par-5* in cell cycle arrest that is induced by DNA damage have been reported in several organisms. These interactions, together with the functional evidence provided in this study, are compiled and depicted in Fig. 7. In yeast, 14-3-3 proteins interact with Chk1 to regulate cell cycle arrest upon DNA damage (Dunaway et al., 2005). Chk1 phosphorylates Wee1, which in turn phosphorylates Cdk1 (Tyr15) to stop the cell cycle (O'Connell et al., 1997), and 14-3-3 proteins are required for proper Chk1 nuclear localization and function (Chen et al., 1999; Dunaway et al., 2005). Therefore, the hypothesis that PAR-5 is necessary for CHK-1 function could explain the defect in CDK-1 phosphorylation and cell cycle arrest after *par-5* knockdown. However, it seems that PAR-5 is not strictly necessary for CHK-1 activation because we observed the CHK-1 active form (phosphorylated at Ser345) and its proper nuclear localization in *par-5(RNAi)* worms (Fig. 3D). Nevertheless, as this observation was carried out in pre-meiotic cells, we cannot rule out a functional interaction between PAR-5 and CHK-1 in proliferating germ cells. Downstream of Chk1, 14-3-3 proteins have been shown to interact with the Cdc25 phosphatase, preventing its interaction with Cdk1 (Peng et al., 1997; Lopez-Girona et al., 1999; Zeng and Piwnica-Worms, 1999). Cdc25 eliminates the Cdk1 (Tyr15) inhibitory phosphorylation (executed by Wee1), thereby allowing Cdk1 to promote progression into mitosis. Therefore, Cdk1 phosphorylation and activity depend on the kinase and phosphatase activities of Wee1 and Cdc25, respectively (O'Connell et al., 2000). Accordingly, our results are compatible with the idea of *par-5* collaborating with *wee-1.3* and counteracting *cdc-25.1* to promote proper cell cycle arrest upon DNA damage. However, *wee-1.3* depletion, in contrast to *par-5*, does not seem to affect germline proliferation in the absence of HU (supplementary material Fig. S8). Therefore, *par-5* functions in the germline are not always coupled with *wee-1.3*.

Finally, 14-3-3 proteins have been shown to regulate Cdk1 localization and function directly (Chan et al., 1999; Laronga et al., 2000; Su et al., 2001). In mammals, phosphorylated Cdk1 is sequestered in the cytoplasm upon DNA damage in a 14-3-3-dependent manner to prevent mitotic catastrophe (Chan et al., 1999). However, in *C. elegans* (similar to yeast), phosphorylated

CDK-1 is located inside the nucleus (Boxem et al., 1999). Therefore, if PAR-5 regulates CDK-1 function, the mechanism should be different from that of cytoplasmic sequestration. Moreover, we showed that PAR-5 is localized in the nucleus upon replication stress, suggesting that the relevant interactions for DDR occur inside the nucleus. Further experiments are needed to identify PAR-5 interactions and their impacts on checkpoint responses and germline proliferation.

C. elegans as a model to study 14-3-3 regulation and function

Although mammalian 14-3-3 homologs have diverged into seven genes, we verified that the basic functions of 14-3-3 in cell cycle control have been conserved in *C. elegans*. Indeed, the mitotic catastrophe observed in *par-5(RNAi)* worms has already been noted in human cells lacking 14-3-3σ after the induction of DNA damage (Chan et al., 1999). However, *C. elegans*, in contrast to mammals, has only one 14-3-3 protein (PAR-5) expressed in the germline, which could explain why *par-5* is essential to maintain the proliferation and genomic stability of the germline. By contrast, the single knockdown of mammalian 14-3-3 has less influence on the cells in the absence of exogenous DNA damage, probably because of functional redundancy (Hermeking and Benzinger, 2006).

DNA fragmentation in the germ cells of *par-5*-knockdown worms treated with different DNA-damaging agents (i.e. CPT, HU or IR) implies the increased sensitivity of proliferating cells to these agents. This observation is in agreement with multiple reports showing that 14-3-3 overexpression is related to chemotherapy resistance in cancer cell lines, and also that 14-3-3 downregulation sensitizes cells to therapy-induced cell death (Porter et al., 2006; Tzivion et al., 2006; Neal and Yu, 2010). Indeed, 14-3-3 proteins have been suggested as possible therapeutic targets in cancer treatment.

Although many studies on 14-3-3 proteins have been published, few have shown the 14-3-3 up- and/or down-regulatory effects in animal models, and most have focused on one isoform (14-3-3σ) (Porter et al., 2006). Hence, the present study paves the way for the use of *C. elegans* as a model to study 14-3-3 functions and expression regulation, and as a high-throughput platform to test new drugs targeting 14-3-3 proteins and to perform genome-wide RNAi screening to identify new 14-3-3 interactors and suppressors.

Materials and Methods
Worm strains and culture conditions
Caenorhabditis elegans strains were cultured and maintained using standard procedures (Stiernagle, 2006). Bristol N2 was used as a WT strain. The following alleles were used during the study: *atl-1(tm853)* (strain DW101); *hus-1(op241) opIs34 [HUS-1:GFP]* (strain WS1433); *par-5(it55)* (strain KK299); *rrf-1(pk1417)* (strain NL2098); and *rrf-3(pk1426)* (strain NL2099). The experiment using the *hus-1(op241)* and *opIs34 [HUS-1:GFP]* was performed at 25°C to maximize the transgene expression. The remaining experiments were carried out at 20°C.

RNAi
To induce RNAi by feeding, nematode growth medium (NGM) plates were supplemented with 100 μg/mL ampicillin, 12.5 μg/mL tetracycline and 3 mM IPTG. The RNAi clones used for the experiments were obtained from either the ORFeome library (Rual et al., 2004) (*par-5*, *mpk-1*, *cdc-25.1* and *wee-1.3*) or the Ahringer library (Kamath et al., 2003) (*par-2* and *par-3*). Plates seeded with the corresponding RNAi clones were used to feed WT synchronized L1 worms (unless another stage is stated). All RNAi clones were verified by sequencing. The WT strain fed with a clone carrying the L4440 empty vector was used as an RNAi negative control.

Germline dissection and quantification
To quantify the cells in the proliferative region, gonads were dissected, fixed (formaldehyde 3%, methanol 75%, K_2HPO_4 6.2 mM) and stained with DAPI (0.6 μg/mL) after the corresponding treatments. The stained gonads were photographed using a Leica DM5000B microscope. Digital pictures were used for germ cell quantification in a single Z stack within 50 μm of the distal end of the gonad. For the germline time-course experiment, germ nuclei from the distal part to the bend of the gonad were scored in a single Z stack. At least 15 germlines were quantified for each experiment.

DDR assays
To perform all the cell cycle arrest assays, L4 stage worms (42–46 hours post-L1) of the corresponding genotypes or RNAi were treated with different DNA-damaging agents. For the HU assay, worms were transferred onto NGM plates containing HU (25 mM; SIGMA, cat # H8627) for 20–24 hours before dissection. For the CPT assay, worms were transferred onto NGM plates containing CPT (40 μM; Sigma-Aldrich, cat # C9911) or DMSO 0.1% for 20–24 hours. The dissected gonads were used for immunostaining with a phosphorylated CDK-1(Tyr15) antibody. For the IR assay, worms were irradiated with γ-rays (120 Gy) using a Cesium137 source (model IBL-437-C H). Dissection was performed 12 hours post-irradiation.

Embryo cell cycle timing
Embryos for video recordings were obtained from worms treated as follows: L4 stage worms, grown at 20°C, were transferred onto plates containing the indicated RNAi or the RNAi empty vector L4440. After 24 hours, half of the adult worms were transferred onto plates containing HU (75 mM). The other half was used as a control. HU-treated embryos were recorded from 5.5 hours to 10 hours after HU treatment. Video recordings were performed using Nomarski optics at 21°C with continuous video acquisition at one frame per second. The cell cycle timing of the first embryonic division was determined as described by Antonia Holway (Holway et al., 2006).

Immunostaining
For immunostaining, adult worms were immobilized in Levamisole 0.3 mM (in PBS). Their gonads were then dissected and fixed in a manner appropriate for the primary antibody. For antibody staining against RAD-51 (a gift from Anton Gartner), gonads were fixed for 10 minutes in PFA 2% (diluted in PBS). For antibody staining against phosphorylated H3 (Ser10) (Millipore, cat. # 04-817) and phosphorylated CDK-1 (Tyr15) (Calbiochem, cat. # 219440), gonads were fixed in FA 3% (diluted in K_2HPO_4 6.2 mM) for 10 minutes. For antibody staining against PAR-5 (a gift from Andy Golden), gonads were fixed for 30 minutes in 2% PFA followed by a post-fixation incubation in cold methanol (5 minutes). Primary antibody dilutions were as follows: RAD-51 (1:200); phosphorylated H3 (1:1000); PAR-5 (1:800); and phosphorylated CDK-1(Tyr15) (1:50). Primary incubations were performed overnight in 0.1% PBS Tween and 1% BSA. After fixation and antibody incubations, gonads were washed three times with PBS Tween 0.1%. A secondary antibody, Alexa-Fluor-568-conjugated goat anti-rabbit antibody (Molecular Probes, Invitrogen) was used to label the gonads. All samples were counterstained with DAPI (0.6 μg/mL) to visualize the nuclei. Staining conditions for phosphorylated CHK-1 (Ser345) (Cell Signaling Technology, cat. # 2348) were as previously described by Se-jin Lee and collaborators (Lee et al., 2010).

Western blotting
Adult worms were washed off plates with M9 buffer and rocked for 30 minutes. They were then washed twice with M9, and the pellets mixed with Lysis buffer 2X (4% SDS, 100 mM Tris-HCl pH 6.8, 20% glycerol, 1 × protease inhibitor cocktail (CalBioChem), 1 mM orthovanadate, 2 mM NaF, 10 mM glycerol 2-phosphate disodium and 500 nM sodium pyrophosphate). Once mixed, the pellets were incubated in boiling water for 15 minutes. The obtained lysates were electrophoresed on SDS 12% polyacrylamide gels and electroblotted onto nitrocellulose membranes. Blotting was carried out using the primary antibodies for PAR-5 (from Andy Golden), tubulin (Developmental Studies Hybridoma Bank, cat. # E7) and secondary horseradish-peroxidase-conjugated anti-rabbit and anti-mouse (DAKO). Primary antibody dilutions were 1:4000 and 1:10,000, respectively.

Quantitative RT-PCR
Adult worms were washed off plates with M9 buffer and rocked for 30 minutes. They were then washed twice with M9, and the pellets were mixed with TRI REAGENT (MRC Technology) to extract RNA following the manufacturer's instructions. For cDNA synthesis, a High Capacity Retro Transcription kit (Applied Biosystems) was used. SYBR-GREEN (Applied Biosystems) reagent was used to perform the amplification reaction followed by a real-time quantification using the ABI PRISM 7500 system. The -fold change expression of the corresponding genes was based on the ddCT method and normalized relative to the amplification obtained using *act-1* (actin) primers. Primer sequences were as follows: *par-5* (FW: ACCGCGTCAAGGTTGAGCAAGA, RV: ACAACGGCA-GCGCGATCCTC); *ftt-2* (FW: TCCGGAGACGACAGAAACTCGGT, RV:

CTGGCAAGCCTTGTCCGGGG); and *act-1* (FW: CCGCTCTTGCCCCATCA-ACCA, RV: CGATGGATGGGCCGGACTCG).

Supplementary material available online at
http://jcs.biologists.org/lookup/suppl/doi:10.1242/jcs.094896/-/DC1

References

Ahmed, S., Alpi, A., Hengartner, M. O. and Gartner, A. (2001). C. elegans RAD-5/CLK-2 defines a new DNA damage checkpoint protein. *Curr. Biol.* **11**, 1934-1944.

Alpi, A., Pasierbek, P., Gartner, A. and Loidl, J. (2003). Genetic and cytological characterization of the recombination protein RAD-51 in Caenorhabditis elegans. *Chromosoma* **112**, 6-16.

Arur, S., Ohmachi, M., Nayak, S., Hayes, M., Miranda, A., Hay, A., Golden, A. and Schedl, T. (2009). Multiple ERK substrates execute single biological processes in Caenorhabditis elegans germ-line development. *Proc. Natl. Acad. Sci. USA* **106**, 4776-4781.

Bailly, A. P., Freeman, A., Hall, J., Déclais, A.-C., Alpi, A., Lilley, D. M., Ahmed, S. and Gartner, A. (2010). The Caenorhabditis elegans homolog of Gen1/Yen1 resolvases links DNA damage signaling to DNA double-strand break repair. *PLoS Genet.* **6**, e1001025.

Berdichevsky, A., Viswanathan, M., Horvitz, H. R. and Guarente, L. (2006). C. elegans SIR-2.1 interacts with 14-3-3 proteins to activate DAF-16 and extend life span. *Cell* **125**, 1165-1177.

Bhalla, N. (2010). Meiotic checkpoints: repair or removal? *Curr. Biol.* **20**, R1014-R1016.

Boxem, M., Srinivasan, D. G. and van den Heuvel, S. (1999). The Caenorhabditis elegans gene ncc-1 encodes a cdc2-related kinase required for M phase in meiotic and mitotic cell divisions, but not for S phase. *Development* **126**, 2227-2239.

Brauchle, M., Baumer, K. and Gönczy, P. (2003). Differential activation of the DNA replication checkpoint contributes to asynchrony of cell division in C. elegans embryos. *Curr. Biol.* **13**, 819-827.

Burrows, A. E., Sceurman, B. K., Kosinski, M. E., Richie, C. T., Sadler, P. L., Schumacher, J. M. and Golden, A. (2006). The C. elegans Myt1 ortholog is required for the proper timing of oocyte maturation. *Development* **133**, 697-709.

Chan, T. A., Hermeking, H., Lengauer, C., Kinzler, K. W. and Vogelstein, B. (1999). 14-3-3Sigma is required to prevent mitotic catastrophe after DNA damage. *Nature* **401**, 616-620.

Chen, L., Liu, T. H. and Walworth, N. C. (1999). Association of Chk1 with 14-3-3 proteins is stimulated by DNA damage. *Genes Dev.* **13**, 675-685.

Collis, S. J., Barber, L. J., Clark, A. J., Martin, J. S., Ward, J. D. and Boulton, S. J. (2007). HCLK2 is essential for the mammalian S-phase checkpoint and impacts on Chk1 stability. *Nat. Cell Biol.* **9**, 391-401.

Dunaway, S., Liu, H.-Y. and Walworth, N. C. (2005). Interaction of 14-3-3 protein with Chk1 affects localization and checkpoint function. *J. Cell Sci.* **118**, 39-50.

Engels, K., Giannattasio, M., Muzi-falconi, M., Lopes, M. and Ferrari, S. (2011). 14-3-3 Proteins regulate exonuclease 1-dependent processing of stalled replication forks. *PLoS Genet.* **7**, e1001367.

Ford, J. C., al-Khodairy, F., Fotou, E., Sheldrick, K. S., Griffiths, D. J. and Carr, A. M. (1994). 14-3-3 protein homologs required for the DNA damage checkpoint in fission yeast. *Science* **265**, 533-535.

Garcia-Muse, T. and Boulton, S. J. (2005). Distinct modes of ATR activation after replication stress and DNA double-strand breaks in Caenorhabditis elegans. *EMBO J.* **24**, 4345-4355.

Gartner, A., MacQueen, A. J. and Villeneuve, A. M. (2004). Methods for analyzing checkpoint responses in Caenorhabditis elegans. *Methods Mol. Biol.* **280**, 257-274.

Hermeking, H. and Benzinger, A. (2006). 14-3-3 proteins in cell cycle regulation. *Semin. Cancer Biol.* **16**, 183-192.

Hofmann, E. R., Milstein, S., Boulton, S. J., Ye, M., Hofmann, J. J., Stergiou, L., Gartner, A., Vidal, M. and Hengartner, M. O. (2002). Caenorhabditis elegans HUS-1 is a DNA damage checkpoint protein required for genome stability and EGL-1-mediated apoptosis. *Curr. Biol.* **12**, 1908-1918.

Holway, A. H., Kim, S.-H., La Volpe, A. and Michael, W. M. (2006). Checkpoint silencing during the DNA damage response in Caenorhabditis elegans embryos. *J. Cell Biol.* **172**, 999-1008.

Jaramillo-Lambert, A., Ellefson, M., Villeneuve, A. M. and Engebrecht, J. (2007). Differential timing of S phases, X chromosome replication, and meiotic prophase in the C. elegans germ line. *Dev. Biol.* **308**, 206-221.

Jaramillo-Lambert, A., Harigaya, Y., Vitt, J., Villeneuve, A. and Engebrecht, J. (2010). Meiotic errors activate checkpoints that improve gamete quality without triggering apoptosis in male germ cells. *Curr. Biol.* **20**, 2078-2089.

Kalogeropoulos, N., Christoforou, C., Green, A. J., Gill, S. and Ashcroft, N. R. (2004). chk-1 is an essential gene and is required for an S-M checkpoint during early embryogenesis. *Cell Cycle* **3**, 1196-1200.

Kamath, R. S., Fraser, A. G., Dong, Y., Poulin, G., Durbin, R., Gotta, M., Kanapin, A., Le Bot, N., Moreno, S., Sohrmann, M. et al. (2003). Systematic functional analysis of the Caenorhabditis elegans genome using RNAi. *Nature* **421**, 231-237.

Killian, D. J. and Hubbard, E. J. (2005). Caenorhabditis elegans germline patterning requires coordinated development of the somatic gonadal sheath and the germ line. *Dev. Biol.* **279**, 322-335.

Kim, J. H., Gelbard, A. S. and Perez, A. G. (1967). Action of hydroxyurea on the nucleic acid metabolism and viability of HeLa cells. *Cancer Res.* **27**, 1301-1305.

Kumagai, A. and Dunphy, W. G. (1999). Binding of 14-3-3 proteins and nuclear export control the intracellular localization of the mitotic inducer Cdc25. *Genes Dev.* **13**, 1067-1072.

Laronga, C., Yang, H. Y., Neal, C. and Lee, M. H. (2000). Association of the cyclin-dependent kinases and 14-3-3 sigma negatively regulates cell cycle progression. *J. Biol. Chem.* **275**, 23106-23112.

Lee, J., Kumagai, A. and Dunphy, W. G. (2001). Positive regulation of Wee1 by Chk1 and 14-3-3 proteins. *Mol. Biol. Cell* **12**, 551-563.

Lee, S.-J., Gartner, A., Hyun, M., Ahn, B. and Koo, H.-S. (2010). The Caenorhabditis elegans Werner syndrome protein functions upstream of ATR and ATM in response to DNA replication inhibition and double-strand DNA breaks. *PLoS Genet.* **6**, e1000801.

Li, J., Tewari, M., Vidal, M. and Lee, S. S. (2007). The 14-3-3 protein FTT-2 regulates DAF-16 in Caenorhabditis elegans. *Dev. Biol.* **301**, 82-91.

Lopez-Girona, A., Furnari, B., Mondesert, O. and Russell, P. (1999). Nuclear localization of Cdc25 is regulated by DNA damage and a 14-3-3 protein. *Nature* **397**, 172-175.

Morton, D. G., Shakes, D. C., Nugent, S., Dichoso, D., Wang, W., Golden, A. and Kemphues, K. J. (2002). The Caenorhabditis elegans par-5 gene encodes a 14-3-3 protein required for cellular asymmetry in the early embryo. *Dev. Biol.* **241**, 47-58.

Moser, S. C., von Elsner, S., Büssing, I., Alpi, A., Schnabel, R. and Gartner, A. (2009). Functional dissection of Caenorhabditis elegans CLK-2/TEL2 cell cycle defects during embryogenesis and germline development. *PLoS Genet.* **5**, e1000451.

Neal, C. L. and Yu, D. (2010). 14-3-3ζ as a prognostic marker and therapeutic target for cancer. *Expert Opin. Ther. Targets* **14**, 1343-1354.

O'Connell, M. J., Raleigh, J. M., Verkade, H. M. and Nurse, P. (1997). Chk1 is a wee1 kinase in the G2 DNA damage checkpoint inhibiting cdc2 by Y15 phosphorylation. *EMBO J.* **16**, 545-554.

O'Connell, M. J., Walworth, N. C. and Carr, A. M. (2000). The G2-phase DNA-damage checkpoint. *Trends Cell Biol.* **10**, 296-303.

Peng, C. Y., Graves, P. R., Thoma, R. S., Wu, Z., Shaw, A. S. and Piwnica-Worms, H. (1997). Mitotic and G2 checkpoint control: regulation of 14-3-3 protein binding by phosphorylation of Cdc25C on serine-216. *Science* **277**, 1501-1505.

Porter, G. W., Khuri, F. R. and Fu, H. (2006). Dynamic 14-3-3/client protein interactions integrate survival and apoptotic pathways. *Semin. Cancer Biol.* **16**, 193-202.

Raleigh, J. M. and O'Connell, M. J. (2000). The G(2) DNA damage checkpoint targets both Wee1 and Cdc25. *J. Cell Sci.* **113**, 1727-1736.

Rual, J.-F., Ceron, J., Koreth, J., Hao, T., Nicot, A.-S., Hirozane-Kishikawa, T., Vandenhaute, J., Orkin, S. H., Hill, D. E., van den Heuvel, S. et al. (2004). Toward improving Caenorhabditis elegans phenome mapping with an ORFeome-based RNAi library. *Genome Res.* **14**, 2162-2168.

Stergiou, L., Doukoumetzidis, K., Sendoel, A. and Hengartner, M. O. (2007). The nucleotide excision repair pathway is required for UV-C-induced apoptosis in Caenorhabditis elegans. *Cell Death Differ.* **14**, 1129-1138.

Stiernagle, T. (2006). Maintenance of C. elegans. *WormBook*, 1-11.

Su, T. T., Parry, D. H., Donahoe, B., Chien, C. T., O'Farrell, P. H. and Purdy, A. (2001). Cell cycle roles for two 14-3-3 proteins during Drosophila development. *J. Cell Sci.* **114**, 3445-3454.

Suzuki, A. and Ohno, S. (2006). The PAR-aPKC system: lessons in polarity. *J. Cell Sci.* **119**, 979-987.

Tzivion, G., Gupta, V. S., Kaplun, L. and Balan, V. (2006). 14-3-3 proteins as potential oncogenes. *Semin. Cancer Biol.* **16**, 203-213.

Wang, W. and Shakes, D. C. (1997). Expression patterns and transcript processing of ftt-1 and ftt-2, two C. elegans 14-3-3 homologues. *J. Mol. Biol.* **268**, 619-630.

Ward, J. D., Barber, L. J., Petalcorin, M. I., Yanowitz, J. and Boulton, S. J. (2007). Replication blocking lesions present a unique substrate for homologous recombination. *EMBO J.* **26**, 3384-3396.

Zeng, Y. and Piwnica-Worms, H. (1999). DNA damage and replication checkpoints in fission yeast require nuclear exclusion of the Cdc25 phosphatase via 14-3-3 binding. *Mol. Cell. Biol.* **19**, 7410-7419.